Distribution of ^{226}Ra in the Arctic Ocean and the Bering Sea and its hydrologic implications

XING Na (邢 娜), CHEN Min (陈 敏), HUANG Yipu (黄奕普), CAI Pinghe (蔡平河) & QIU Yusheng (邱雨生)

Department of Oceanography, Xiamen University, Xiamen 361005, China
Correspondence should be addressed to Xing Na (email: x_nacn@yahoo.com.cn)

Received August 7, 2002

Abstract Radium-226 (^{226}Ra) activities were measured in the surface water samples collected from the Arctic Ocean and the Bering Sea during the First Chinese National Arctic Research Expedition. The results showed that ^{226}Ra concentrations in the surface water ranged from 0.28 to 1.56 Bq/m^3 with an average of 0.76 Bq/m^3 in the Arctic Ocean, and from 0.25 to 1.26 Bq/m^3 with an average of 0.71 Bq/m^3 in the Bering Sea. The values were obviously lower than those from open oceans in middle and low latitudes, indicating that the study area may be partly influenced by sea ice meltwater. In the Bering Sea, ^{226}Ra in the surface water decreased northward, probably as a result of the exchange between the ^{226}Ra-deficient sea ice meltwater and the ^{226}Ra-rich Pacific water. In the Arctic Ocean, ^{226}Ra in the surface water increased northward and eastward. This spatial distribution of ^{226}Ra reflected the variation of the ^{226}Ra-enriched river component in the water mass of the Arctic Ocean. The vertical profiles of ^{226}Ra in the Canadian Basin showed a concentration maximum at 200 m, which could be attributed to the inputs of the Pacific water or/and the bottom shelf water with high ^{226}Ra concentration. This conclusion was consistent with the results from ^{2}H, ^{18}O tracers.

Keywords: Arctic Ocean, Bering Sea, ^{226}Ra, distribution.

The Arctic Ocean, the northernmost parts of the earth, covers the total surface area of 14.79 million square kilometers and amounts to only about 4% of global ocean surface area. Although its surface area is the smallest in the four major oceans, the Arctic Ocean plays an important role in the regulation of global climate, material balance and energy circulation of global ecosystem. The Arctic Ocean has seasonal or long-term ice cover, extended periods of darkness during the Arctic winter and the wide continental shelves covering about 36% of the total surface area of the Arctic Ocean, a percentage unparalleled by other oceans. These unique features have led to the recent interest in the hydrology of the Arctic Ocean.

The major water inputs to the Arctic Ocean are the Atlantic water, river water, and the Pacific-originated water entering through the Bering Strait. The Atlantic water is characterized by its high salinity and temperature. The high freshwater component in Arctic surface water, to a large extent, is due to river runoff to the Arctic Basin, which amounts to 10% of global river discharge[1]. Additional freshwater inputs come from sea ice meltwater and precipitation. Among the freshwater components of the Arctic surface water, sea ice meltwater and meteoric water can be distin-

guished with $d\ ^{18}O$[2]. Both silicate and alkalinity were used as tracers to distinguish the contribution of the Pacific water through the Bering Strait [3].

The upper halocline water between 50 and 200 m of the Arctic Basin, which is characterized by a constant temperature at most the freezing point and a salinity that increases with depth, has interested many oceanographers. Jones and Anderson[4] showed that the upper halocline water is associated with a maximum in silicate, phosphate, nitrate, normalized total carbonate and a minimum in oxygen at the CESAR Ice Station (81°43.4′N, 93°25′W). Moore and Smith[5] showed that this layer also had a maximum in ^{226}Ra and a minimum in ^{210}Pb at this station. Temperature, salinity, NO/PO ratio, ^{2}H and ^{18}O tracers have been used to investigate the sources and mechanism of the upper halocline water.

^{226}Ra (half-life = 1622 a) has been successfully used to study circulation and mixing of the ocean water masses. It was suggested that ^{226}Ra, just like ^{14}C, was an ideal naturally occurring radionuclide for water movement in the ocean. With the implementation of several international research plans, such as GEOSECS, WOCE, and JGOFS, ^{226}Ra activities in the world oceans have been determined extensively. However, very few data about ^{226}Ra in the Arctic Ocean and the Bering Sea have been reported. Tsunogai and Harada[6] determined ^{226}Ra and ^{210}Pb activities in the samples collected from four stations in the Bering Sea, and found that a maximum in ^{226}Ra occurred in mid-depth waters. Moore and Smith[5] studied the disequilibria among ^{226}Ra, ^{210}Pb and ^{210}Po at the CESAR Ice Station (81°43.4′N, 93°25′W), and found that the ^{226}Ra activities increased to a maximum at depths corresponding to the nutrients maximum and upper halocline. By measuring ^{222}Rn and ^{226}Ra in the southeastern Bering Sea shelf waters and sediments, Glover and Reeburgh[7] pointed out that the ^{226}Ra activities showed a heterogeneous distribution in the southeastern Bering Sea shelf and a positive correlation with dissolved silicate.

In this study, thirty-three surface water samples and twelve vertical samples were collected from the Arctic Ocean and the Bering Sea during the First Chinese National Arctic Research Expedition conducted from July to September in 1999. The spatial distribution of ^{226}Ra in surface waters gave information about the influence of sea ice meltwater on ^{226}Ra activities. The relationship between ^{226}Ra activities and dissolved silicate concentrations was evaluated. In addition, the vertical profiles of ^{226}Ra were used to provide clues to the possible sources of the upper halocline water in the Canadian Basin.

1 Methods

1.1 Sample location

During the First Chinese National Arctic Research Expedition (from July to September in 1999), 13 and 20 large-volume surface water samples were collected in the Arctic Ocean and the Bering Sea, respectively (fig. 1). Sampling stations covered the Chukchi Sea (9 stations), the Beaufort Sea (Station C30 and Station C33), the Canadian Basin (Station C34 and Station C39), the western Bering Sea (18 stations) and the Norton Sound (Station BJ10).

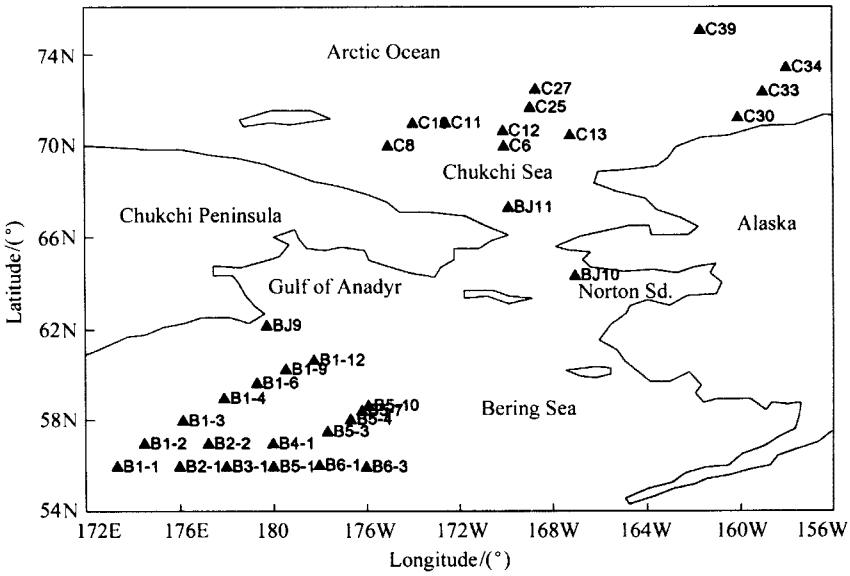

Fig. 1. Location of sampling stations in the Arctic Ocean and the Bering Sea.

1.2 Sample collection

120 dm^3 surface water samples were collected and passed through a PVC pipe packed with the MnO_2-impregnated fibers. Flow rate was controlled at 200—250 cm^3/min in order to absorb radium isotopes quantitatively. After the enrichment, MnO_2-fibers were taken out and enveloped using plastic bags. The fibers were taken back to the onshore laboratory for ^{226}Ra measurement.

Vertical samples at Station C34 and Station C39 in the Canadian Basin were obtained by hanging MnO_2-fibers at different depths. After certain hours, MnO_2-fibers were taken out and enveloped using plastic bags. The fibers were taken back to the shore-based laboratory.

1.3 Methodology

1.3.1 ^{226}Ra analysis. In the laboratory, MnO_2-fibers were taken out from the plastic bags. Residual waters in the fibers were removed. The fibers were filled into a diffusion tube, which was subsequently sealed and vacuumized. After 5—7 d, when ^{222}Rn ingrown reached a significant level, a vacuumized scintillation counting cell was sequentially connected to the diffusion tube packed with MnO_2-fibers and an airflow adjustor. ^{222}Rn was emanated from MnO_2-fibers into the counting cell for 15 min. After sealing in the cell for 3 h, ^{222}Rn will be in equilibrium with his daughters. The activities were subsequently measured by using a Rn-Th analyzer (FD-125)[8].

The specific activity of ^{226}Ra, A_{226}, was calculated from the following equation:

$$A_{226} = \frac{k_{226}(N_s - N_b)}{a \cdot V \cdot h \cdot t},$$

where A_{226} is the specific activity of ^{226}Ra in the water sample (Bq/m^3), k_{226} is the counting coefficient for ^{226}Ra (Bq/cpm), N_s and N_b are the total counts of the sample and the background respec-

tively (with a consistent counting time t), a is the ingrown coefficient of ^{222}Rn; V is the sample volume (m^3), h is the emanation efficiency of ^{222}Rn from MnO_2-fibers, t is the counting time of the sample and the background (min).

1.3.2 Influence of residual water in MnO_2-fibers upon ^{226}Ra measurement. In our laboratory, the aforementioned method for ^{226}Ra measurement has been set up for many years. However, the procedure for removing residual water in MnO_2-fibers was different for different samples. In order to check the influence of this procedure on ^{226}Ra measurement, five vertical samples from Station C34 were selected for measuring ^{226}Ra in MnO_2-fibers and residual water. The residual water in the fibers was extruded by pressure and collected completely. ^{226}Ra in MnO_2-fibers and residual waters were determined by the radon emanation method aforementioned. These results (table 1) showed that ^{226}Ra activities in residual water were considerably lower than those in MnO_2-fibers. Among the five samples, ^{226}Ra activities in the residual water of three samples were below the detection limit. In the other samples, ^{226}Ra activities were detectable but lower than those in MnO_2-fibers by 3 orders of magnitude. The results provided the evidence showing that ^{226}Ra contents in the extruded waters were negligible and the method used for ^{226}Ra determination was reliable.

Table 1 ^{226}Ra activities in MnO_2-fibers and residual water from Station C34

Sample layer/m	$\frac{^{226}Ra}{V} \times 10^2$/Bq · m^{-3} a)	Residual water	$\frac{^{226}Ra}{V} \times 10^2$/Bq · m^{-3} a)
25	3.04 ± 0.06	L-C34-25 m	B.D[b)]
50	4.49 ± 0.07	L-C34-50 m	0.09 ± 0.07
100	3.99 ± 0.06	L-C34-100 m	B.D[b)]
200	4.65 ± 0.07	L-C34-200 m	0.07 ± 0.07
500	2.44 ± 0.06	L-C34-500 m	B.D[b)]

a) Assuming that the water volume flowing through MnO_2-fiber is V (in dm^3); b) B.D, below the detection limit.

1.4 Analysis of other parameters

Temperature and salinity were determined *in-situ* via MARK III C/WOCE-CTD. Nutrients were analyzed according to the national standards in China "Marine Investigation Criteria · Measurement of Chemical Parameters in Seawater" (GB1276-4-01). NO_3^- data were calibrated for zinc reduction efficiency[9].

2 Results and discussion

2.1 ^{226}Ra activities in the surface seawater

^{226}Ra activities in 33 surface seawater samples collected from the Arctic Ocean and the Bering Sea are listed in table 2. The results showed that ^{226}Ra activities in the surface waters ranged from 0.28 to 1.56 Bq/m^3 with an average of 0.76 Bq/m^3 in the Arctic Ocean, and from 0.25 to 1.26 Bq/m^3 with an average of 0.71 Bq/m^3 in the Bering Sea. Our results were consistent with previous

Table 2 ^{226}Ra specific activities in the surface seawaters from the Arctic Ocean and the Bering Sea

Sea area	Station	Longitude	Latitude	Depth/m	Salinity (‰)	^{226}Ra/Bq · m^{-3}
Arctic Ocean	C6	170°0.6′W	69°59.9′N	50	25.633	0.28 ± 0.02
	C8	174°59.5′W	70°0.7′N	60	31.147	0.34 ± 0.02
	C10	173°54.3′W	71°0.1′N	35	26.669	0.43 ± 0.03
	C11	172°29.6′W	71°1.3′N	38	30.500	0.28 ± 0.03
	C12	170°2.1′W	70°40.1′N	30	30.520	1.17 ± 0.04
	C13	167°10.2′W	70°28.8′N	50	31.021	1.31 ± 0.04
	C25	168°52.6′W	71°42.0′N	50	29.099	0.28 ± 0.03
	C27	168°38.2′W	72°29.6′N	54	30.291	1.56 ± 0.04
	C30	160°0.6′W	71°15.3′N	44	29.850	0.52 ± 0.03
	C33	158°56.5′W	72°22.5′N	50	28.395	0.87 ± 0.04
	C34	157°55.9′W	73°25.2′N	2700	26.409	1.19 ± 0.04
	C39	161°55.3′W	75°16.1′N	2080	28.295	0.94 ± 0.03
	BJ11	169°49.5′W	67°18.7′N	47	31.852	0.91 ± 0.04
Bering Sea	BJ9	179°45.9′E	62°11.2′N	–	31.708	0.60 ± 0.02
	BJ10	166°59.6′W	64°21.8′N	–	26.987	0.78 ± 0.03
	B1-12	178°14.2′W	60°39.7′N	165	32.168	0.33 ± 0.03
	B1-9	179°25.8′W	60°15.2′N	840	32.665	0.29 ± 0.03
	B1-6	179°19.7′E	59°39.6′N	3200	32.730	0.42 ± 0.03
	B1-4	177°55.4′E	58°59.4′N	3720	32.848	0.26 ± 0.04
	B1-3	176°9.4′E	58°0.2′N	3780	32.968	0.46 ± 0.02
	B1-2	174°30.5′E	56°59.8′N	3650	33.011	1.22 ± 0.04
	B1-1	173°21.1′E	55°59.8′N	3850	32.970	0.60 ± 0.03
	B2-1	176°0.6′E	56°0.1′N	3860	32.821	1.26 ± 0.04
	B3-1	177°59.8′E	56°0.0′N	3860	32.972	0.76 ± 0.03
	B5-1	179°59.1′W	55°59.9′N	3830	32.768	0.76 ± 0.04
	B6-1	178°1.2′W	56°2.8′N	3780	32.932	0.25 ± 0.02
	B6-3	175°59.9′W	55°59.5′N	3720	32.866	0.72 ± 0.04
	B5-3	177°39.3′W	57°31.3′N	3680	32.906	1.09 ± 0.05
	B4-1	180°0.0′W	56°59.9′N	3810	32.832	0.62 ± 0.03
	B2-2	177°14.0′E	56°59.7′N	3830	32.996	0.85 ± 0.04
	B5-4	176°39.5′W	58°3.6′N	3370	32.688	1.19 ± 0.05
	B5-7	176°10.8′W	58°26.0′N	2440	32.628	0.95 ± 0.05
	B5-10	175°53.9′W	58°39.9′N	139	32.409	0.83 ± 0.04

data from the Arctic Ocean and the Bering Sea, but obviously lower than those from open oceans in middle and lower latitudes (table 3).

The low ^{226}Ra activities in the study area may be caused by sea ice meltwater. Sea ice is composed of pure-water ice, seawater and air packed in ice when the temperature is higher than –8.2℃. When the temperature is equal to –8.2℃, $Na_2SO_4 \cdot 10H_2O$ can be crystallized and separated out. $NaCl \cdot 2H_2O$ can be separated out after the temperature decreases to –22.9℃. Other salts will be congealed entirely at –55℃. During the formation of sea ice, the fractionation of ^{226}Ra may occur and result in the low ^{226}Ra activities in sea ice and the high activities in saline waters. Besides, ^{226}Ra activities in the snow covering on the sea ice could be low. Both effects will

result in low ^{226}Ra contents in sea ice meltwater. Unfortunately, there has not been any data reported about ^{226}Ra activities in the sea ice at present.

Table 3 ^{226}Ra activities in the surface water from different sea areas

Sea area	^{226}Ra/Bq · m^{-3} a)	Reference
Pacific Ocean	Average ≈1.07	[10]
Atlantic Ocean	Average ≈1.23	[11]
Indian Ocean	1.30—2.28(16)	[12]
Western Pacific Ocean	1.30—1.40(2)	
Indonesian Sea	1.38—2.77(6)	
Nansha Sea Area	1.57(1)	
Amazon Estuary	0.83—3.62(20)	[13]
Dead Sea (100—300 m)	1153—1927(14)	[14]
East China Sea, Yellow Sea	0.95—3.33(31)	[15]
Seto Inland Sea	0.22—3.07(82)	[16]
Orinoco Estuary	0.48—2.99(22)	[17]
Jiulongjiang Estuary	2.10—5.92(11)	[18]
Bering Sea(KH-75-4)	^{226}Ra (salinity(‰))	[6]
Station 8(57°00′N,171 °00′E)	1.50 ± 0.13(32.83)	
Station 9(57°00′N,174 °54′E)	1.73 ± 0.13(33.17)	
Station 10(57°01′N, 179°03′E)	1.00 ± 0.07(32.95)	
Station 11(57°05′N, 177°05′W)	1.03 ± 0.10(32.53)	
Arctic Ocean(CESAR Station)	1.78 (depth: 25 m)	[5]
Eastern Bering Sea	~0.33—~1.67	[7]
Arctic Ocean	0.28—1.56	this study
Bering Sea	0.25—1.26	

a) Except for particular annotation, the values in the brackets are the sample numbers.

2.2 Spatial distribution of ^{226}Ra and other parameters in the surface seawater——the composition of the water masses in the Arctic Ocean

Spatial distributions of temperature, salinity and nutrients (NO_3^-, PO_4^{3-}, SiO_3^{2-}) in the surface water are shown in fig. 2(a)—(e). Surface temperature in the study area decreased northward. The distribution of surface salinity was relatively complicated. In the Bering Sea, surface salinity increased westward. In the Arctic Ocean, salinity in the surface water decreased in the offshore direction and reached the minimum (25.633‰) at Station C6 in the middle region. This distribution pattern indicated that the freshwater composition in the Arctic Ocean increased in the offshore direction and converged at the internal region. The spatial distribution of nutrients (nitrate, phosphate and silicate) in the surface water had a similar feature: nutrient concentrations decreased northward in the Bering Sea and increased northward and formed a high concentration area in the middle region of Arctic Ocean.

Spatial distribution of ^{226}Ra activities in the surface water of the Arctic Ocean and the Bering Sea is shown in fig. 3. In the Bering Sea, ^{226}Ra in the surface water decreased northward, probably as a result of the exchange between the ^{226}Ra-deficient sea ice meltwater and the ^{226}Ra-rich Pacific water. In the Arctic Ocean, ^{226}Ra in the surface water increased northward and eastward,

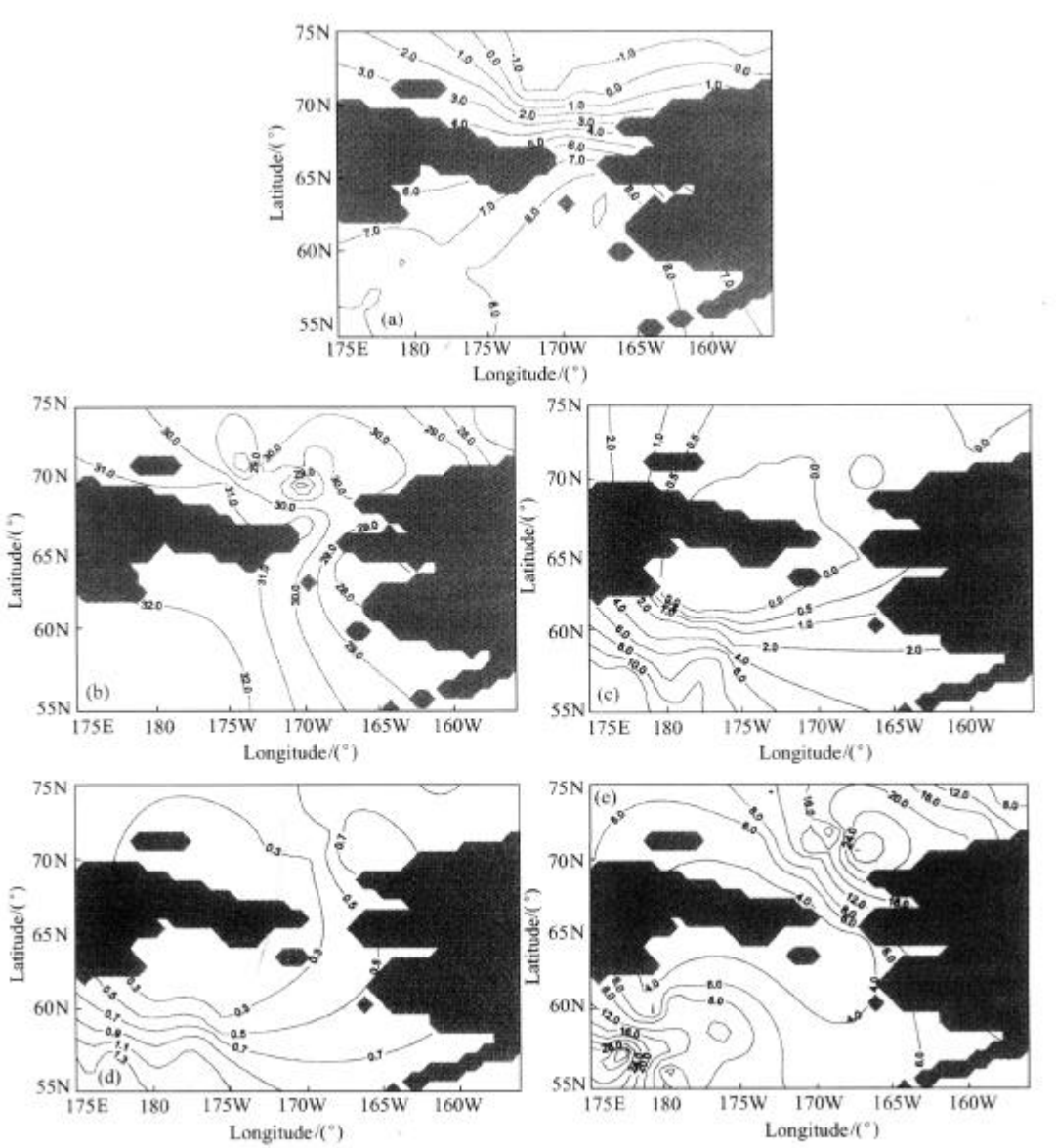

Fig. 2. Spatial distributions of various parameters in the surface water. (a) Temperature (℃); (b) salinity (‰); (c) nitrate (μmol/m^3); (d) phosphate (μmol/m^3); (e) silicate (μmol/m^3).

and formed a high concentration area in the internal region. Since river water carried not only "original" dissolved ^{226}Ra, but also the ^{226}Ra released from suspended particles by desorption, it had a high ^{226}Ra characteristic. The distribution pattern of ^{226}Ra thus indicated that the river component increased in the offshore direction and converged at the internal ocean. Additionally, since continental shelves covered about 1/3 of the total surface area of the Arctic Ocean and most water inputs had a long residence time on the shelves before entering the internal ocean, the hydrogra

phy of the Arctic Ocean was strongly influenced by these extensive shelf areas[19]. Thus, river water and shelf water with high ^{226}Ra converged at the internal Arctic Ocean. The distribution of ^{226}Ra in the study area showed a unique pattern, contrary to the general pattern in which ^{226}Ra decreased in the offshore direction. The information about water mass composition obtained from the spatial distribution of ^{226}Ra was coincident with that of the results from salinity and ^{2}H, ^{18}O tracers[20].

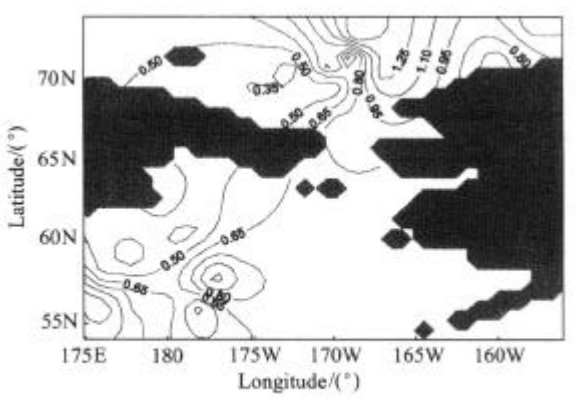

Fig. 3. Spatial distribution of ^{226}Ra activities in the surface water.

Although the spatial distributions of ^{226}Ra activities and salinities indicated the similar information on the water mass composition in the Arctic Ocean, there was no statistically significant linear relationship between ^{226}Ra activity and salinity. This was mainly due to the interstitial water input from bottom sediment. In addition, sea ice meltwater with low salinity may also contribute to the insignificant linear relationship between ^{226}Ra and salinity.

2.3 Correlation between ^{226}Ra activity and dissolved silicate concentration

Both ^{226}Ra activities and dissolved silicate concentrations decreased northward in the Bering Sea and increased northward in the Arctic Ocean and formed a high concentration region in the internal Arctic Ocean (fig. 3 and fig. 2(e)). Linear regression showed that ^{226}Ra activities had a statistically significant positive correlation with dissolved silicate concentrations (fig. 4, correlation coefficient was 0.52 at the 99% confidence level). Glover and Reeburgh[7] also explored the relationship between ^{226}Ra activities and dissolved silicate for all samples collected from the southeastern Bering Sea, and found a significant positive linear relationship between ^{226}Ra and silica at the 95% confidence level (correlation coefficient is 0.66).

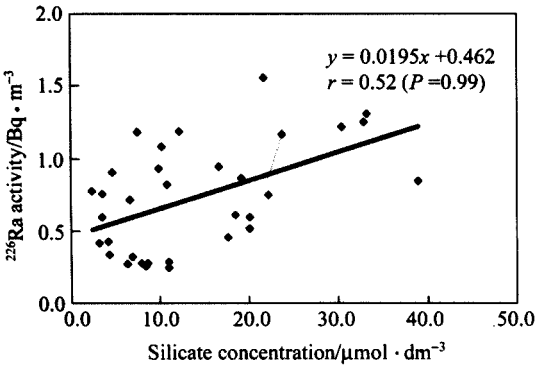

2.4 Profiles of ^{226}Ra in the Canadian Basin——sources and mechanism for the upper halocline water

Vertical samples in the upper water between 0 and 500 m were collected by hanging MnO_2-fibers at certain depths for several hours at Station C34 and Station C39 in the Canadian

Basin. Because of no data about the water volume flowing through MnO_2-fibers, ^{226}Ra activities cannot be calculated quantitatively. However, taking into account the fact that the MnO_2-fibers drifted continually with the ship during sampling and the drift velocity far exceeded the horizontal flow rate of waters, it is reasonable to assume that the flow rate at each depth was similar and the water volume through MnO_2-fibers is consistent. Thus, ^{226}Ra relative activities can be calculated. The results are listed in table 4.

Table 4 ^{226}Ra relative activities at two stations in the Canadian Basin

Station	Depth/m	Temperature/℃	Salinity (‰)	$\frac{^{226}Ra}{V} \times 10^2$/Bq · m^{-3} a)
C34 (157°55.9′W, 73°25.2′N)	25	–1.100	29.616	3.04 ± 0.06
	50	–1.016	31.769	4.49 ± 0.07
	100	–1.510	32.522	3.99 ± 0.06
	150	–1.509	33.040	4.08 ± 0.07
	200	–0.974	33.975	4.65 ± 0.07
	500	0.470	34.823	2.44 ± 0.06
C39 (161°55.3′W, 75°16.1′N)	25	–0.944	29.382	0.57 ± 0.03
	50	–0.732	31.642	1.14 ± 0.04
	100	–1.396	32.590	1.56 ± 0.04
	200	b)	b)	1.93 ± 0.05
	300	0.410	34.694	1.43 ± 0.05
	500	0.569	34.823	2.02 ± 0.05

a) Assuming that the water volume flowing through MnO_2-fiber is V/dm^3; b) no data.

The profiles of ^{226}Ra and other parameters at the two stations (C34 and C39) in the Canadian Basin are shown in figs. 5 and 6. The results showed that the water columns had the characteristic of "the upper halocline water" with a constant temperature of at most the freezing point and a salinity that increases with depth (figs. 5(a) and 6(a)). Nitrate, phosphate and silicate had maximal concentrations at depths of 150—200 m (figs. 5(b) and 6(b)). Conservative parameters NO and PO had maximums at 200 m and minimums at 300 m, while NO/PO ratio had a minimum at 200 m. The ratio increased distinctly from this depth and kept almost constant below 300 m (figs. 5(c) and 6(c)). Corresponding with these hydrochemical characteristics, ^{226}Ra showed a concentration maximum at 200 m (figs. 5(d) and 6(d)). The maximum could be attributed to the inputs of the Pacific water or/and the bottom shelf water with a high ^{226}Ra concentration. The results based on ^{226}Ra were supported by those from ^2H, ^{18}O tracers[21].

Aagaard et al.[21] proposed two possibilities for the maintenance of the upper halocline water: the first is that it was maintained by the lateral advection of cold, saline water formed by sea ice formation on the continental shelves; the second is that it was formed by the upwelling and cooling of the Atlantic layer during winter. Moore and Smith[5] argued that this water mass had its origin in the Bering Sea, but was strongly modified during its residence on the shelf, especially by

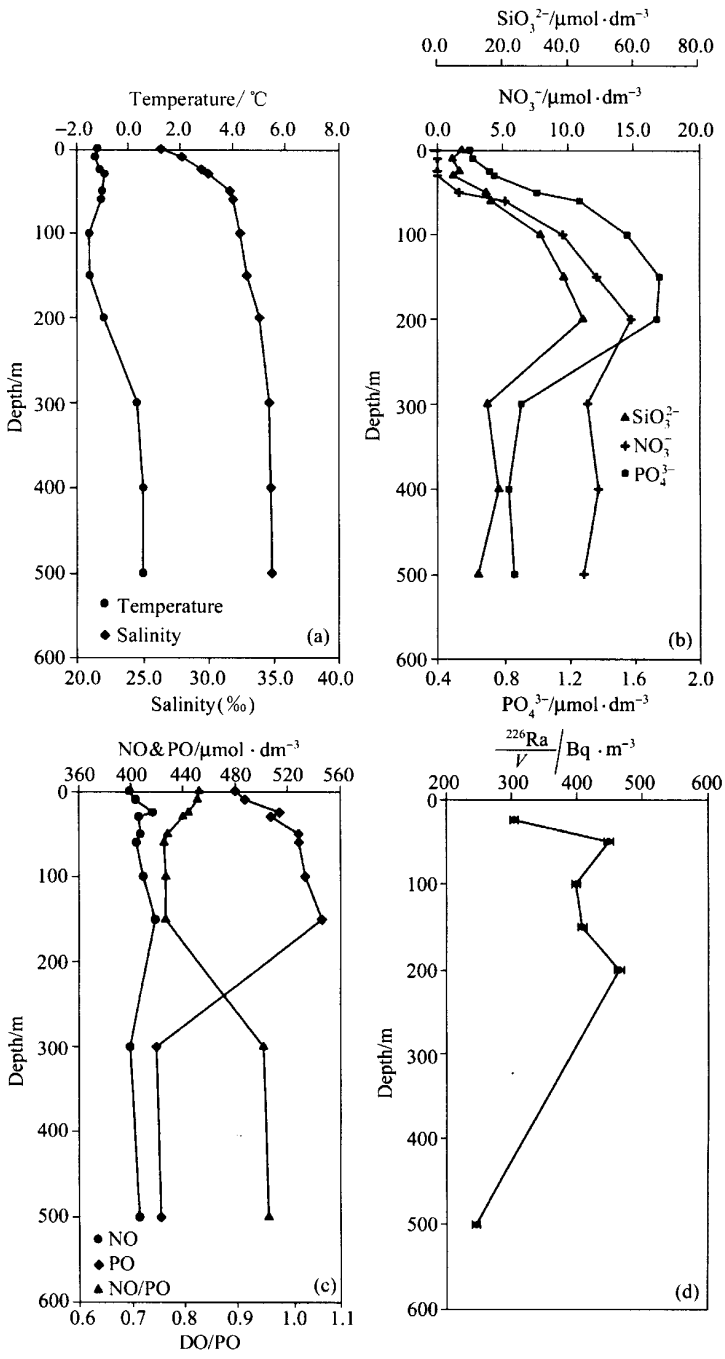

Fig. 5. The vertical profiles of ^{226}Ra and other parameters at Station C34. (a) Temperature (●) and salinity (◆); (b) nitrate (+), phosphate (■) and silicate (▲) (μmol/m^3); (c) NO (●), PO (◆) (μmol/m^3) and NO/PO (▲); (d) ^{226}Ra specific activity (Bq/m^3).

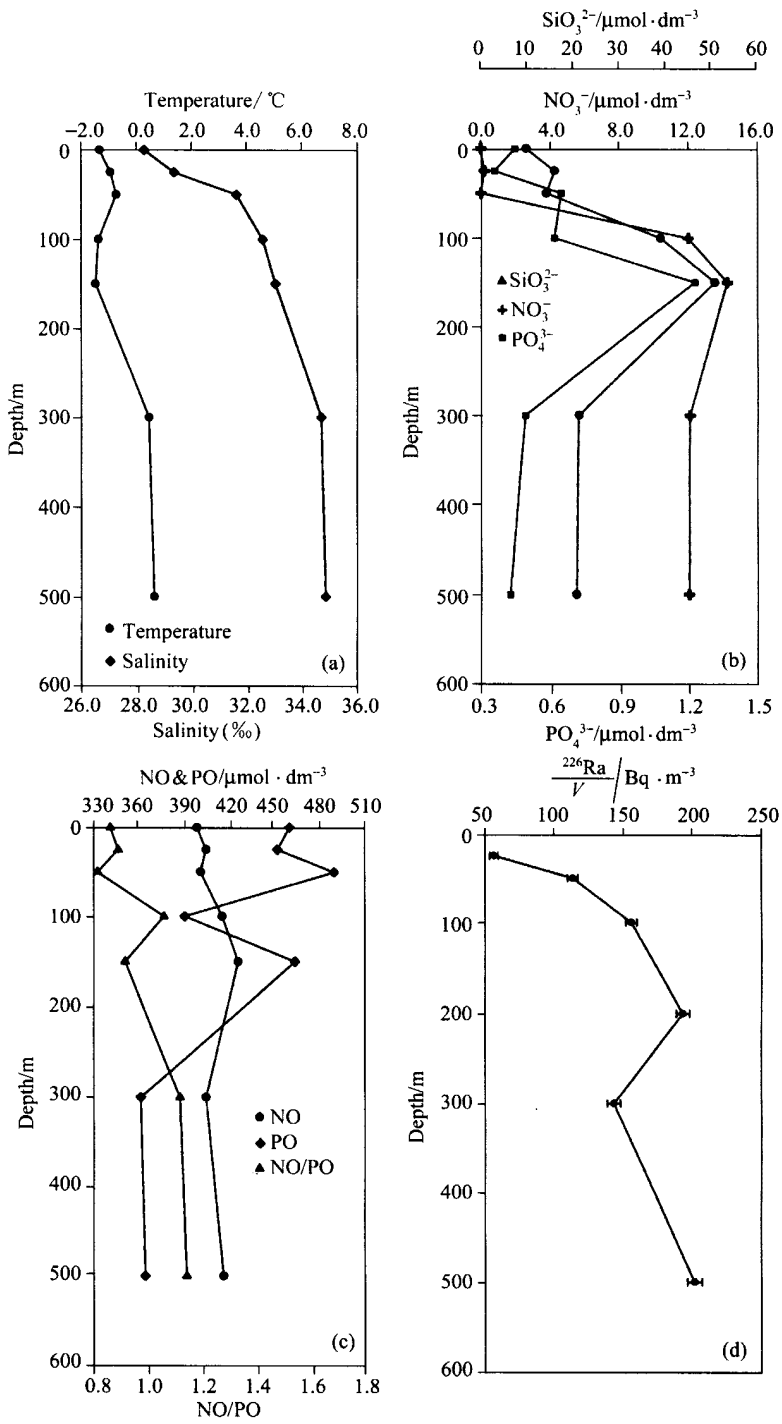

Fig. 6. The vertical profiles of ^{226}Ra and other parameters at Station C39. (a) Temperature (℃) and salinity (‰); (b) nitrat phosphate and silicate (μmol/m^3); (c) NO, PO (μmol/m^3) and NO/PO; (d) ^{226}Ra specific activity (Bq/m^3). Designators are th same as in fig. 5.

the halocline water. They analyzed the distribution of NO/PO data in the Arctic Ocean and over the shelves and concluded that the upper halocline water must be derived from the Pacific Ocean surface water, which was modified on the Chukchi/Bering shelf. Bauch et al.[23] developed a 4-component model to determine the contribution of river water, meltwater, Atlantic Ocean and Bering Strait inflows, using d^{18}O, salinity and silicate as tracers. Applied to the data from CESAR Ice Station, their model reproduces the high proportion of Bering Strait Inflow in the upper halocline water. The results presented above were in agreement with our present understanding of the sources and mechanism of the upper halocline water in the Canadian Basin, primarily based on ^{226}Ra profiles.

Note that ^{226}Ra also had a maximum at 500 m at Station C39 (fig. 6(d)). Similar phenomenon was also observed in the profile of ^{228}Ra. This phenomenon has not been explained reasonably and is worthy of further research.

3 Conclusions

(1) ^{226}Ra activities in the surface water ranged from 0.28 Bq/m^3 to 1.56 Bq/m^3 with an average of 0.76 Bq/m^3 in the Arctic Ocean, and from 0.25 Bq/m^3 to 1.26 Bq/m^3 with an average of 0.71 Bq/m^3 in the Bering Sea. These values were obviously lower than those from open oceans in middle and lower latitudes, indicating that the study area may be partly influenced by sea ice meltwater.

(2) In the Bering Sea, ^{226}Ra in the surface water decreased northward, probably as a result of the exchange between the ^{226}Ra-deficient sea ice meltwater and the ^{226}Ra-rich Pacific water. In the Arctic Ocean, surface ^{226}Ra increased northward and eastward. This spatial distribution of ^{226}Ra reflected the variation of the ^{226}Ra-enriched river component in the water mass of the Arctic Ocean.

(3) Profiles of ^{226}Ra in the Canadian Basin showed a concentration maximum at depth of 200 m. The maximum could be attributed to the inputs of the Pacific water or/and the bottom shelf water with high ^{226}Ra concentration.

In brief, ^{226}Ra distribution in the Arctic Ocean and Bering Sea has a unique pattern compared to that of other sea areas. These features can be used to study the water inputs in the Arctic Ocean, to evaluate the sources and mechanism of the upper halocline water in the internal Arctic Basin, and to quantify the exchange between the Arctic Ocean and the northern Pacific Ocean. Furthermore, it will be helpful to understanding the regulation of Chinese and global climates.

Acknowledgements The authors are indebted to the officers and crew of "Xue Long" Polar Research Vessel of China for their assistance during sample collection. They appreciate Jiao Yutian, an engineer of the First Institute of Oceanography of the State Oceanic Administration, and associate professor Gao Guoping of the Ocean University of Qingdao for their providing the temperature and salinity data. We thank Jin Mingming and Lu Yong of the Second Institute of Oceanography of the State Oceanic Administration, who provided us with nutrient data. We also acknowledge three reviewers for their comments and criticisms, which greatly improved our manuscript. This work was supported by the First Chinese National Arctic Research Expedition Program.

References

1. Aagaard, K., Carmack, E. C., The role of sea ice and other fresh water in the Arctic Ocean, Journal of Geophysical Research, 1989, 94: 14485—14498.
2. Östlund, G., Hut, G., Arctic Ocean water mass balance from isotope data, Journal of Geophysical Research, 1984, 89: 6373—6381.
3. Anderson, L. G., Björk, G., Holby, O. et al., Water masses and circulation in the Eurasian Basin: Results from the Oden 91 expedition, Journal of Geophysical Research, 1994, 99: 3273—3283.
4. Jones, E. P., Anderson, L. G., On the origin of the chemical properties of the Arctic Ocean halocline, Journal of Geophysical Research, 1986, 91: 10759—10767.
5. Moore, R. M., Smith, J. N., Disequilibria between ^{226}Ra, ^{210}Pb and ^{210}Po in the Arctic Ocean and the implications for chemical modification of the Pacific water inflow, Earth and Planetary Science Letters, 1986, 77: 285—292.
6. Tsunogai, S., Harada, K., ^{226}Ra and ^{210}Pb in the Western North Pacific, in Isotope Marine Chemistry (eds. Goldberg, E. D., Yoshio, H., Katsuko, S.), Tokyo: Uchida Rokakuho Pub. Co., LTD; Chinese ed. by Huang Yipu, Shi Wenyuan, Zou Hanyang et al., Beijing: China Ocean Press, 1990, 102—117.
7. Glover, D. M., Reeburgh, W. S., Rn-222 and Ra-226 in southeastern Bering Sea shelf waters and sediment. Continental Shelf Research, 1987, 7(5): 433—456.
8. Xie, Y., A study on radium isotopes geochemical in South China Sea and Xiamen adjacent sea area (in Chinese), Ph.D thesis, Xiamen University, Xiamen, China, 1994, 1—91.
9. Jin, M., Dang, R., A study on nutrient reduction efficiency in the zinc and cadmium reduction method (in Chinese), in Abstracts for Meeting of Marine Technology and Marine Resource Development in 21st Century, Shanghai: Chinese Oceanography Society, 2001, 22.
10. Chung, Y., A deep Ra-226 maximum in the northeast Pacific, Earth and Planetary Science Letters, 1976, 32: 249—257.
11. Broecker, W. S., Goddard, J., Sarmiento, J. L., The distribution of ^{226}Ra in the Atlantic Ocean, Earth and Planetary Science Letters, 1976, 32: 220—235.
12. Okubo, T., Furuyama, K., Sakanoue, M., Distribution of ^{228}Ra in the surface sea water of the East Indian Ocean, Geochemical Journal, 1979, 13: 201—206.
13. Key, R. M., Stallard, R. F., Moore, W. S. et al., Distribution and flux of ^{226}Ra and ^{228}Ra in the Amazon River Estuary, Journal of Geophysical Research, 1985, 90: 6995—7004.
14. Chan, L. H., Chung, Y., Barium and radium in the Dead Sea, Earth and Planetary Science Letters, 1987, 85: 41—53.
15. Nozaki, Y., Tsubota, H., Kasemsupaya, V. et al., Residence times of surface water and particle-reactive ^{210}Pb and ^{210}Po in the East China and Yellow Seas, Geochimica Cosmochimica Acta, 1991, 55: 1265—1272.
16. Kasemsupaya, V., Tsubota, H., Nozaki, Y., ^{228}Ra and its implications in the Seto Inland Sea, Estuarine Coastal and Shelf Science, 1993, 36: 31—45.
17. Moore, W. S., Todd, J. F., Radium isotopes in the Orinoco Estuary and Eastern Caribbean Sea, Journal of Geophysical Research, 1993, 98: 2233—2244.
18. Xie, Y., Huang, Y., Shi, W. et al., ^{226}Ra and ^{228}Ra in Jiulongjiang estuary area, Journal of Oceanography in Taiwan Strait (in Chinese), 1994, 13: 394—399.
19. Rutgers van der Loeff, M. M., Key, R. M., Scholten, J. et al., ^{228}Ra as a tracer for shelf water in Arctic Ocean, Deep-Sea Research II, 1995, 42(6): 1533—1553.
20. Chen, M., Huang, Y., Cai, P., Water mass and movement in the Arctic Ocean based on ^{2}H, ^{18}O tracers, Abstracts for Meeting of Marine Technology and Marine Resource Development in the 21st Century (in Chinese), Shanghai: Chinese Oceanography Society, 2001, 67.
21. Aagaard, K., Coachman, L. K., Carmack, E. C., On the halocline of the Arctic Ocean, Deep-Sea Research, 1981, 28A(6): 529—545.
22. Wilson, C., Wallace, D. W. R., Using the nutrient radio NO/PO as a tracer of continental shelf waters in the central Arctic Ocean, Journal of Geophysical Research, 1990, 95(C12): 22193—22208.
23. Bauch, D., Schlosser, P., Fairbanks, R., Freshwater balance and the sources of deep and bottom waters in the Arctic Ocean inferred from the distribution of $H_2{}^{18}O$, Progress in Oceanography, 1995, 35: 53—80.